

HOSTED BY



ELSEVIER

Contents lists available at ScienceDirect

## Engineering Science and Technology, an International Journal

journal homepage: <http://www.elsevier.com/locate/jestch>

Full Length Article

# Wavelet-fuzzy speed indirect field oriented controller for three-phase AC motor drive – Investigation and implementation

Sanjeevikumar Padmanaban <sup>a,\*</sup>, Febin J.L. Daya <sup>b</sup>, Frede Blaaajerg <sup>c</sup>, Patrick W. Wheeler <sup>d</sup>, Pawel Szcześniak <sup>e</sup>, Valentin Oleschuk <sup>f</sup>, Ahmet H.Ertas <sup>g</sup>

<sup>a</sup> Ohm Technologies, Research and Development, Chennai 600 122, India

<sup>b</sup> School of Electrical Engineering, VIT University, Chennai 600 127, India

<sup>c</sup> Department of Energy Technology, Aalborg University, Pontoppidanstraede 101, 9220 Aalborg, Denmark

<sup>d</sup> Power Electronics, Machines and Control Group, Department of Electrical & Electronics Engineering, Nottingham University, Nottingham NG7 2RD, UK

<sup>e</sup> Institute of Electrical Engineering, University of Zielona Góra, Licealna 9, 65417 Zielona Góra, Poland

<sup>f</sup> Institute of Power Engineering, Academy of Science of Moldova, Chishinev 2028, Moldova

<sup>g</sup> Department of Biomedical Engineering, Engineering Faculty, Karabuk University, Balıkkar Kayasi Mevkii, 78050 Karabuk, Turkey

## ARTICLE INFO

## Article history:

Received 25 July 2015

Received in revised form

12 November 2015

Accepted 12 November 2015

Available online

## Keywords:

Speed compensator

Induction motor

AC drives

Indirect vector control

Wavelet transform

Fuzzy logic

Neural network

## ABSTRACT

Three-phase voltage source inverter driven induction motor is used in many medium- and high-power applications. Precision in speed of the motor play vital role, i.e. popular methods of direct/indirect field-oriented control (FOC) are applied. FOC is employed with proportional–integral (P-I) or proportional–integral–derivative (P-I-D) controllers and they are not adaptive, since gains are fixed at all operating conditions. Therefore, it needs a robust speed controlling in precision for induction motor drive application. This research paper articulates a novel speed control for FOC induction motor drive based on wavelet-fuzzy logic interface system. In specific, the P-I-D controller of IFOC which is actually replaced by the wavelet-fuzzy controller. The speed feedback (error) signal is composed of multiple low and high frequency components. Further, these components are decomposed by the discrete wavelet transform and the fuzzy logic controller to generate the scaled gains for the indirect FOC induction motor. Complete model of the proposed ac motor drive is developed with numerical simulation Matlab/Simulink software and tested under different working conditions. For experimental verification, a hardware prototype was implemented and the control algorithm is framed using TMS320F2812 digital signal processor (dsp). Both simulation and hardware results presented in this paper are shown in close agreement and conformity about the suitability for industrial applications.

Copyright © 2015, The Authors. Production and hosting by Elsevier B.V. on behalf of Karabuk University. This is an open access article under the CC BY-NC-ND license (<http://creativecommons.org/licenses/by-nc-nd/4.0/>).

## 1. Introduction

In industrial application, sectors utilize three-phase induction motor (IM), characterized by the freedom of variable speed control, ruggedness, less maintenance, low cost, reliability, and better efficiency than its counter single-phase IM. Mostly renowned speed controlling techniques are field oriented control (FOC) either indirect or/direct vector control. Such controlling technique produces the decoupling effect of the torque and flux components leading to independent control like dc machines [1]. But still posses drawbacks by its proportional-integral (P-I) or proportional-integral-

derivative (P-I-D) controllers, where their gain values are set constant at all operating conditions. Moreover, the performance of these controllers depends on the slip calculation, which in-turn depends on rotor time constant, and its value depends on the operating condition. Overall, these controllers are not adaptive and less reliable with respect to the environmental conditions of the ac motor drive system.

Controlling techniques of IM are extended by the intelligent techniques like neural network and fuzzy logic found attention and said to overcome the above stated drawbacks [2]. Neural network controller (NNC) does not involve analytical model of the complete system under test and has the ability to adapt it to change in control environment. It is a tedious job to select right neural controller architecture and its training neuron process, and causes increased computation time which affects system performance in real time. Moreover, fuzzy logic controller (FLC) is the simplest intelligent

\* Corresponding author. Tel.: +91-98431-08228.

E-mail address: [sanjeevi\\_12@yahoo.co.in](mailto:sanjeevi_12@yahoo.co.in) (S. Padmanaban).

Peer review under responsibility of Karabuk University.

<http://dx.doi.org/10.1016/j.jestch.2015.11.007>

2215-0986/Copyright © 2015, The Authors. Production and hosting by Elsevier B.V. on behalf of Karabuk University. This is an open access article under the CC BY-NC-ND license (<http://creativecommons.org/licenses/by-nc-nd/4.0/>).

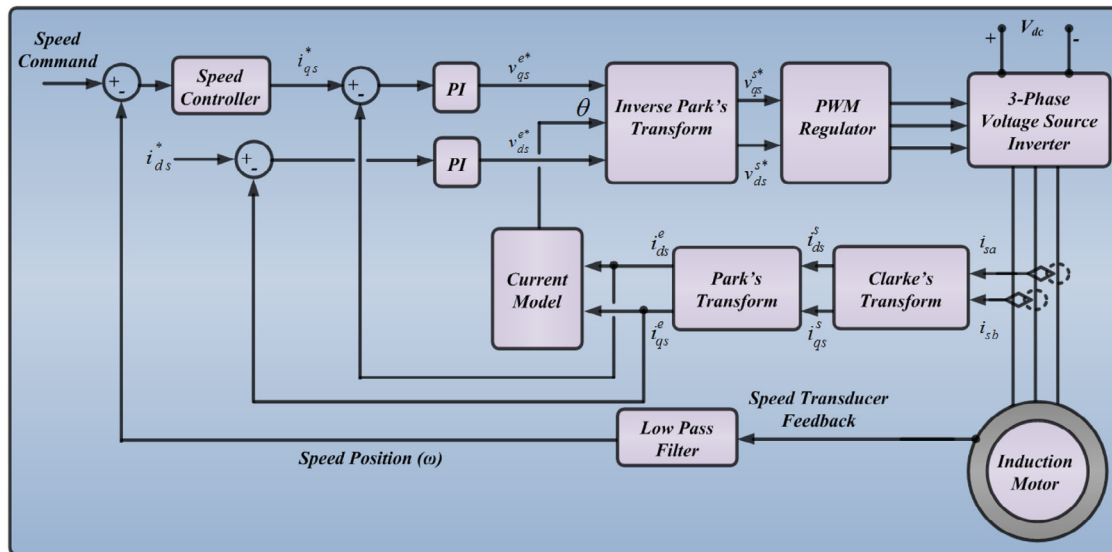


Fig. 1. Configuration of indirect field oriented control (IFOC) scheme for induction motor driven by voltage source inverter (VSI).

version, and its expert knowledge to drive and control the set action works well even if the system is undefined and even subject to parametric variations [2].

Recent years, the wavelet transform (WT) found its application in control systems as well as for fault diagnostics tool for ac motor drives and modulator multilevel converters and transform technique widely popularized [2–12]. Classically, the WT is a multi-resolution spectrum used to extract and detect components of the signal frequencies at any interval by protecting the data and representing it in another form. Neural network with wavelet systems are used to control a servo IM drive [2], where the wavelet neural network controller (WNNC) is designed to implement a computed-torque control technique, and is expected to recover the residual approximation. WNNC based adaptive speed control for a permanent-magnet synchronous motor (PMSM) is addressed, and results show attractive performances [3–5]. Wavelet network (WN) speed controller is also adapted for a dc motor, where the function of WN is an adaptive speed control to achieve high precision [5]. Most complex applications of estimating the rotor time constant for IFOC IM drive are implemented and wavelet application justified by its outcomes by accurate estimations than standard filters [6]. Wavelet modulated inverter for single-phase IM drive, where PWM are generated by non-dyadic wavelet function based on multi-resolution analysis (MRA) is articulated for its applicability in modulation schemes of drives [7].

Complete descriptive survey confirms that there is a recent trend in wavelet transform controller for electric drives. This work articulates on a novel and simple wavelet, fuzzy integrated IFOC speed controller for IM drive. Complete proposed model of the Wavelet-fuzzy IFOC IM drive is developed in numerical (Matlab/Simulink) simulation software and tested under different designed conditions. Further, experimental hardware prototype was built using TMS320F2812 digital signal processor (dsp) for verifying the performances in real time. Set of both simulation and experimental results are provided in this paper, which always shows the effectiveness and reliability of proposed control scheme for industrial application needs.

This paper is organized as follows. Section 2 describes the dynamics of three-phase IM. The discrete wavelet transform is described in section 3. The selection of wavelet and level of decomposition are discussed in section 4. The detailed description about the hardware implementation of the proposed concept, com-

plete set of numerical simulation and experimental results are given in section 5. Finally, the conclusions of this research paper are given in section 6.

## 2. Dynamics of three-phase induction motor

The model of a three-phase voltage source inverter (VSI) driven IM in synchronously rotating (d–q) reference frame of the IFOC IM drive is elaborated in Fig. 1 as schematic diagram [13,14]. It is driven by voltage source inverter (VSI), further the set reference speed (command) of the motor is compared with natural speed (actual) of the motor, thus obtained speed-error-signal given has input to the speed control algorithm. The speed regulator generates reference torque (command) in terms of its current component and thus the q-axis reference current  $i_{qs}^*$  of the IM drive. The reference currents are compared with their respective actual (flux producing) d- and q-axis currents (torque producing), which are actually obtained by the transformation of the stator currents. The respective error signals generate the voltage commands  $v_{ds}^{e*}$  and  $v_{qs}^{e*}$  by the P-I regulators, and these signals are transformed into stationary reference frame voltages  $v_{ds}^{s*}$  and  $v_{qs}^{s*}$ . Now, obtained signals are used for generating the switching signals for the pulse width modulator (PWM) three-phase voltage source inverter (VSI), and the rotor flux position is determined by the current model, hence the slip speed.

## 3. Discrete wavelet transformation algorithm

The wavelet transform (WT) is fast execution math series representation for processing and analysis of given signals. Both time and frequency domains investigation can be carried out [8–11], WT is the extended method of fourier transforms, where the multidimensional time–frequency domain presentation is allowed. The window sizes in short time fourier transform (STFT) are fixed to a limited value while the window size can vary in WT [8]. Moreover, the WT has ability to concentrate the energy of the processed signal in to finite number of coefficients, and they are capable of providing the time frequency localization of the signal [2,8–16]. The mathematical representation of a signal given by WT is as follows [9]:

$$\omega t(\tau, s) = \frac{1}{s} \int x(t) \Psi^* \left( \frac{t-\tau}{s} \right) dt \quad (1)$$

where,  $s > 0$  depicts the window size, which determines resolution of the graded wavelet base  $\psi(t - \tau/s)$  in time–frequency domains. The value of  $s$  parameter is inversely depended on frequency, and the discrete wavelet transform (DWT) of a signal  $x(t)$  is written as below:

$$WT_{m,n} x(t) = \int_{-\infty}^{\infty} x(t) \Psi_{m,n}^*(t) dt \quad (2)$$

where,  $\Psi^*(t)$  is the wavelet function,  $m$  is the dilation representation, and  $n$  is the translational parameter. DWT are realized through cascaded stages of low-pass filter (LPF) and high-pass filter (HPF), followed by down sampling and which performs frequency dilation. The output from the LPF is the approximation signal coefficients at first level of decomposition represented by  $a^1$ . The output from the HPF is the detailed signal coefficients at first level of decomposition represented by  $d^1$ . The coefficients  $a^1$  and  $d^1$  constitute the first level of decomposition and mathematically represented as [13–18]:

$$a^1[n] = \sum_{k=0}^{N-1} g[k] x[n-k] \quad (3)$$

$$d^1[n] = \sum_{k=0}^{N-1} h[k] x[n-k] \quad (4)$$

The approximation coefficient  $a^1$  at first level of decomposition is given as input to the filters after down sampled by two. The second level LPF and HPF generate the second level approximation and coefficient of length  $N/2$ . Second level in decomposition is expressed as below:

$$a^2[n] = \sum_{k=0}^{N/2-1} g[k] a^1[2n-k] \quad (5)$$

$$d^2[n] = \sum_{k=0}^{N/2-1} h[k] a^1[2n-k] \quad (6)$$

To note, the filtering and down sampling process is continued until the desired level is reached.

#### 4. Selection of wavelet and level of decompositions

Operating systems draw different frequency depending on its nature due to the physical and electrical noises interfered with it. The feedback control systems are intended to minimize such noises and destructive signals by minimizing the error-signal in each cycle. Most of the mathematical methods and series representations lack to eliminate noises. The wavelet based controller can perform extremely well by discriminating such signals into different frequency bands.

Control system aspects when wavelet is used are required to select appropriate wavelet function and mother wavelet with scaling function (application dependent). More appropriate selection of wavelet function exactly parameterizes and expands the signal. It also decomposes and reconstructs the signal using the shifted and dilated version of the wavelet function. Desirable properties of the wavelet function are compactness, orthogonality, linear phase, low approximation error, etc [18]. The compactness property of the wavelet function has the advantage of lesser computational efforts. It also detects the frequency components present in the signal, which can be used in the design of speed compensator for the motor drive. The minimal description length (MDL) data criterion best suits the

selection of optimum wavelet function [18]. MDL selects the best wavelet filter for the signal decomposition. According to MDL criterion, the best model within a group of models will have the shortest description of data model itself and defined as [18,19]:

$$MDL(k, n) = \min \left\{ \frac{3}{2} k \log N + \frac{N}{2} \log \|\tilde{\alpha}_n - \alpha_n^{(k)}\|^2 \right\} \quad (7)$$

$0 \leq k < N; \quad 1 \leq n \leq M$

where,  $k$  and  $n$  are the indices. Integer  $N$  states the length of the signal while  $M$  expresses the wavelet filters.  $\tilde{\alpha}_n$  is the wavelet vector, obtained from the transformed coefficients of the signal using the wavelet filter.  $\alpha_n^{(k)} = \Theta^k$ ,  $\tilde{\alpha}_n$  defines the vector containing  $k$  non-zero elements. The threshold parameter  $\Theta^k$ , keeps  $k$  number of largest element in  $\tilde{\alpha}_n$  and sets other all elements to zero. The MDL criterion gives the minimum value for the number of coefficients  $k$ , hence considered as the optimum one.

It is important to select the level of decomposition before applying the error-signal to DWT. The number of decomposition level decides the numbers of tuning gains needed for the wavelet controller and depends on signal used for decomposition. Shannon entropy criterion best suits to determine the optimum level of decomposition of the speed-error-signal for motor drive applications. The entropy of a signal  $x(n)$  and length  $N$  can be represented as:

$$H(x) = - \sum_{n=0}^{N-1} |x(n)|^2 \log |x(n)|^2 \quad (8)$$

The entropy calculation will be performed at every level of decomposition for both approximate and detailed coefficients of the transformed signal. It is used for detecting the optimum level of decomposition. By Shannon entropy based criterion, if the entropy of the signal in the next level ( $p$ ) is higher than the previous ( $p-1$ ), then is expressed below as:

$$H(x)_p \geq H(x)_{p-1} \quad (9)$$

Now, the decomposition of signals can be stopped at level ( $p$ ), i.e. represents the optimum level of decomposition.

In case of classical P-I-D controller, the  $u$  is the manipulated output variable obtained after processing the error-signal  $e$ , where  $e$  obtained from difference of the reference signal (command) and actual signal. The controller output  $u$  of a P-I-D controller is expressed as below:

$$u = k_p e + k_i \int e dt + k_d \frac{de}{dt} \quad (10)$$

where  $k_p$ ,  $k_i$ , and  $k_d$  are gain constants and acts on the error-signal as shown in eq. (9). To be noted, in frequency domain the proportional gain  $k_p$  corresponds to the low frequency component, the integral gain  $k_i$  corresponds to medium frequency component, and the derivative gain  $k_d$  corresponds to high-frequency component of the given error-signal [15]. The same operation is performed by DWT to decompose the given signal to detail and approximate coefficients at different levels of resolution. The manipulated output of the wavelet transform is similar to P-I-D, and calculated from the detail and approximate coefficients as given below [13]:

$$u_w = k_{d1} e_{d1} + k_{d2} e_{d2} + \dots + k_{dN} e_{dN} + k_{aN} e_{aN} \quad (11)$$

where,  $e_{d1}$ ,  $e_{d2}$ , ...,  $e_{dN}$  the detail components and  $e_{aN}$  the approximate component of the given error-signal. The gains  $k_{d1}$ ,  $k_{d2}$ , ...,  $k_{dN}$  is used to tune the detail components and  $k_{aN}$  is used to tune the approximate component of the error-signal [4,20–25]. Two levels of decomposition are sufficient for effective representation of the error signal. The components (low/high frequency components) were

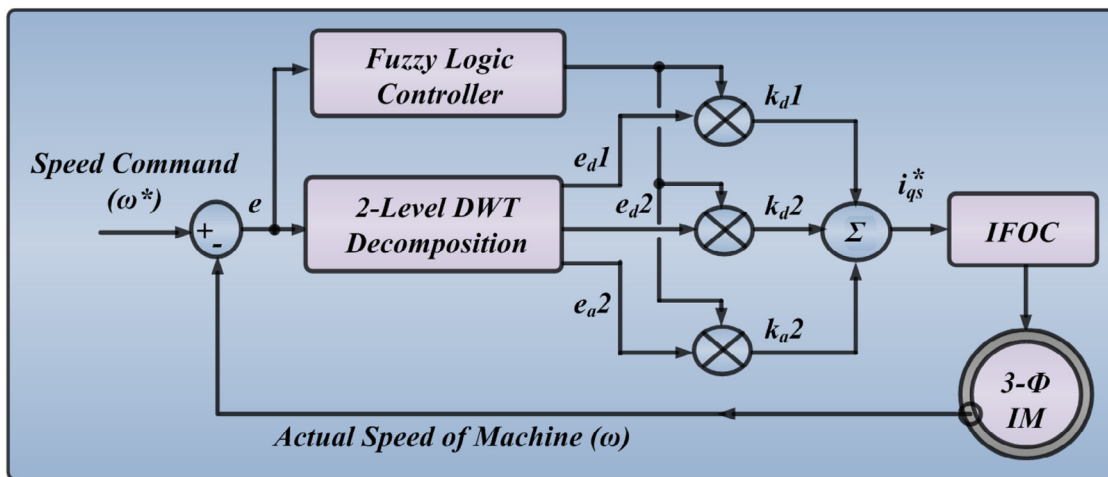
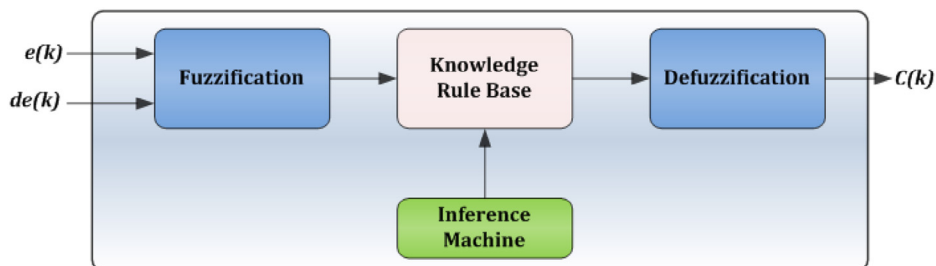


Fig. 2. Schematic of the proposed wavelet-fuzzy based speed compensator for IFOC IM drive.

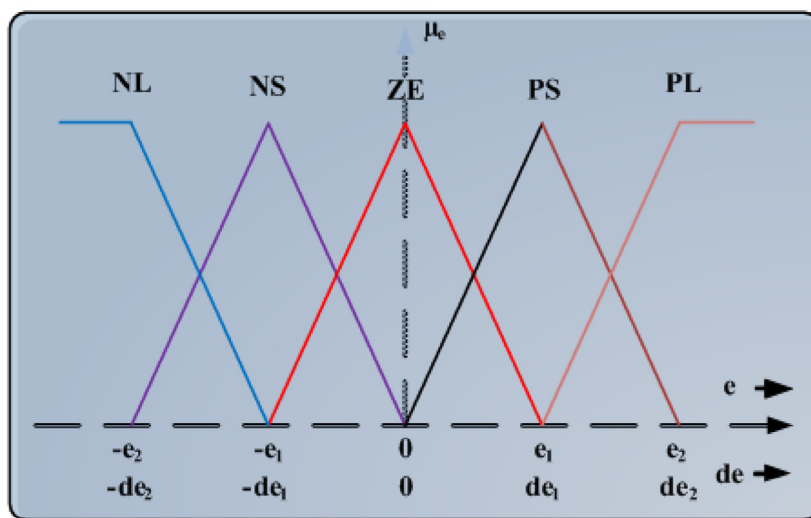
scaled by their respective gains and then added together to generate the control signal  $u$  given by Eq. (11) to robust under all perturbation conditions. Obviously minimum two levels were needed for computation purposes since the first level, which makes the WT equivalent to a low-pass filter, behaves similar to PID version and loses the robustness.

In case of IM drives, the command and disturbances occur at low frequencies, sensor noises at high frequency. The gain which corresponds to low frequency components of the error-signal is used to improve the disturbance rejection of IM. The gain which corre-

sponds to high frequency components of the error-signal is set to minimum for eliminating the effect of noise signal injected to the system [16,25]. A schematic representation of the wavelet-fuzzy based speed control of IFOC IM drive is shown in Fig. 2. The speed-error, which is the difference between the set reference speed (command) and feedback speed (actual), is applied as input to both the WT and fuzzy logic systems. The DWT decomposes the speed-error into the approximate and detail components up to level-two, the respective frequency components ( $e_{d1}$ ,  $e_{d2}$ , and  $e_{a2}$ ). The FLC operates on the speed-error and generate the scaling gains ( $k_{d1}$ ,  $k_{d2}$ ,



(a)



(b)

Fig. 3. (a) Fuzzy logic rule based system generalized structure. (b) Membership functions of the fuzzy logic controller for both, the error (e), and the change-in-error (de).

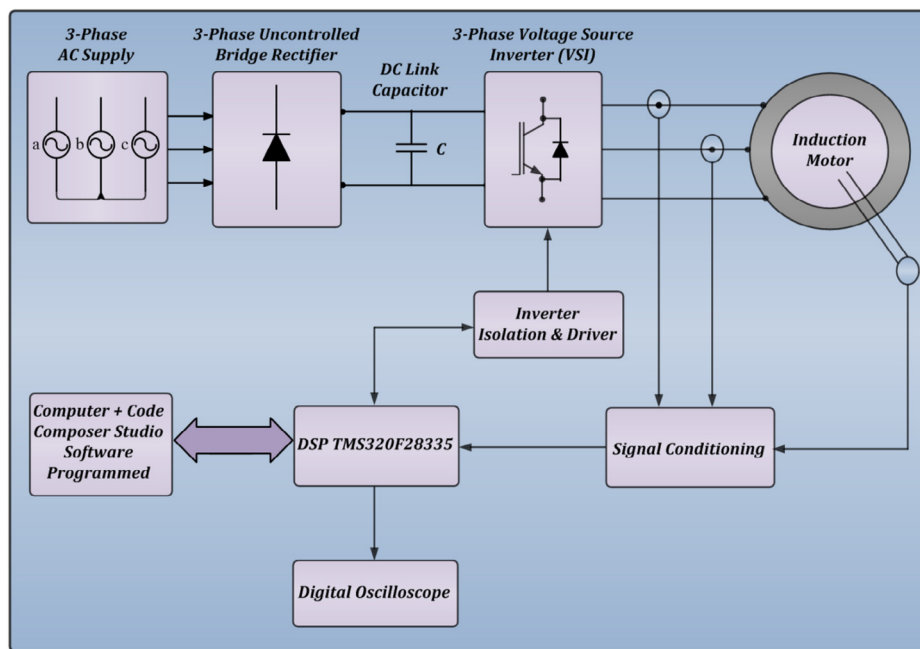
**Table 1**

Matrix formulation (5x5) for fuzzy logic rules.

$de(k)$	$e(k)$				
	NL	NS	ZE	PS	PL
NL	NL	NL	NL	NS	ZE
NS	NL	NL	NS	ZE	PS
ZE	NL	NS	ZE	PS	PL
PS	NS	ZE	PS	PL	PL
PL	ZE	PS	PL	PL	PL

and  $k_{a2}$ ). Further, these scaling gains are combined (multiplied) with the corresponding wavelet coefficients to generate the electromagnetic torque component command for the IM drive. The torque component command generated by the wavelet-fuzzy controller is used to perform the IFOC IM drive and schematically illustrated by Fig. 2.

Fig. 3(a) shows the schematic illustration of the FLC system, it consists of fuzzy interface, fuzzy rules, and de-fuzzification units. The inputs to the FLC are the speed-error and the change in speed-error (difference between present speed-error and its immediate previous state), correspondingly the membership functions shown are in Fig. 3(b). In first step of FLC, using the triangular membership functions as given by Fig. 3(b) converts the crisp variables  $e(k)$  and  $de(k)$  into fuzzy variables such as  $E(k)$  and  $dE(k)$ . Each universe of discourse further divided into five fuzzy sets has: NL (negative-large), NS (negative-small), ZE (zero), PS (positive-small), and PL (positive-large). Each fuzzy variable is the subset member with a degree of membership varying between zero (non-member) and one (full-member). In the second step of FLC, the fuzzy variables  $E(k)$  and  $dE(k)$  are processed by an inference engine that executes a set of control rules contained (5 × 5) matrix given by Table 1 [2,17–19,22–24]. These rules are designed based on the dynamic behavior of the error signal, resulting in symmetrical matrix,



(a)



(b)

**Fig. 4.** Experimental prototype implementation of wavelet-fuzzy IFOC speed controller for IM drive. (a) Schematic of the proposed wavelet-fuzzy based speed compensator for IFOC IM drive, (b) Laboratory setup for the real time implementation of the proposed speed compensator scheme.

**Table 2**  
Main parameters of AC motor drive.

Rated power	2	[hp]
Rated voltage	460	[V]
Rated frequency	60	[Hz]
Rated speed	1750	[rpm]
Number of pole pairs	2	
Stator resistance	2.12	[ $\Omega$ ]
Rotor resistance	2.08	[ $\Omega$ ]
Stator Inductance	5.97	[mH]
IGBT single module (total 6 units for 3-phase VSI)	IRG7PG35UPbF, $V_{CES} = 1000V$ , $I_c = 35A$ , $T_c = 100C$ , $T_{J(Max)} = 175C$ , $V_{CE(ON)}$ typ. = 1.9V@ $I_c = 20A$	
DC link capacitor	1200V/1000 $\mu$ F	

and these are general rule-based design with a 2-D phase plane. Each rule is expressed in the form:

**If 'x' is 'A' and 'y' is 'B' then 'z' is 'C'.**

Different inference algorithms can be used to space the fuzzy set values for the output fuzzy variable  $c(k)$ , in this work, the max-min inference algorithm is used. In which the membership degree is equal to the maximum of the product between  $E$  and  $dE$  membership degree. The output variable from the inference engine is then converted into a crisp value in the de-fuzzification stage. Again, various de-fuzzification algorithms have been proposed in the literature, but in this work the centroid de-fuzzification algorithm is used. In which the crisp value is calculated from the centre of gravity of the membership function. The definition of the spread of each partition, or conversely, the width and symmetry of the membership functions is generally a compromise between dynamic and

steady state accuracy. Equally spaced partitions and consequently symmetrical triangles are reasonable choices [18,19] and considered in this work. The input variables are fuzzified using five membership functions normalized between +1/-1.

In the next section, experimental prototype setups, complete set of simulation and experiment tests results are provided along in the discussion.

## 5. Experimental prototype setup, numerical simulation and experimental test results

Fig. 4(a) illustrates the proposed wavelet-fuzzy speed control IFOC IM drive as schematic block diagram. Fig. 4(b) shows the complete laboratory prototype hardware, it mainly consists of software controlled PC, TMS320F2812 (dsp) board, IGBT based PWM inverter and signal (voltage/current) measuring instruments. The

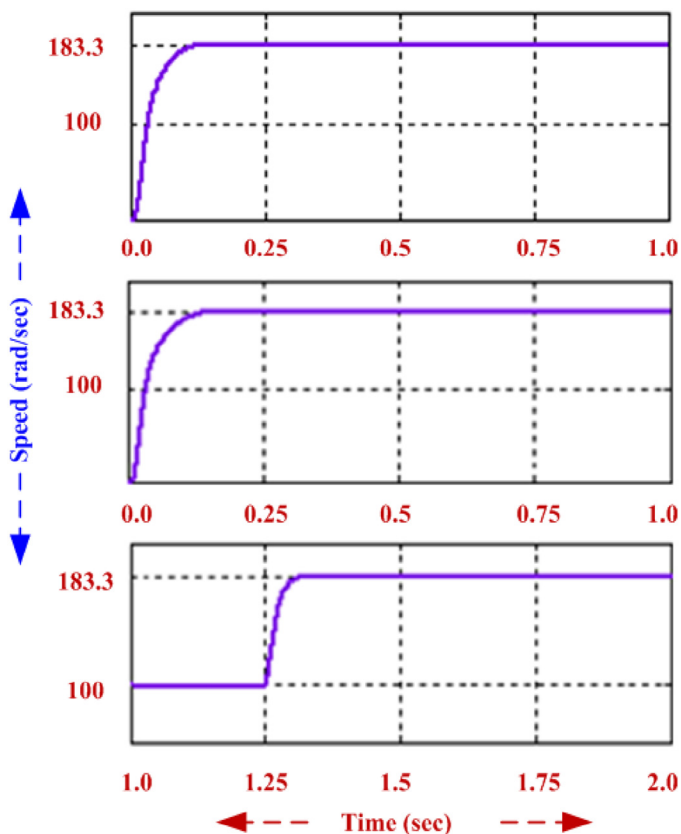


**Fig. 5.** Numerical simulation test, speed behavior of the induction motor controlled by the wavelet-fuzzy IFOC. **Top:** starting at no-load with set speed command 183.3 rad/sec, **Middle:** starting at loaded condition of 2.5 Nm (set speed 183.3 rad/sec), **Bottom:** no-load with step increase in set speed command 100-183.3 rad/sec at  $t = 1.25$  sec.

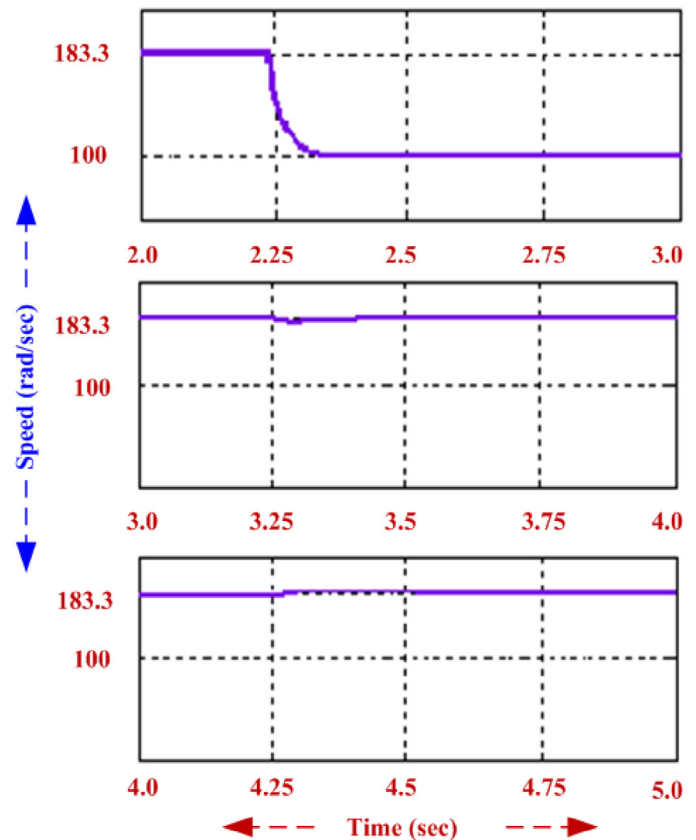
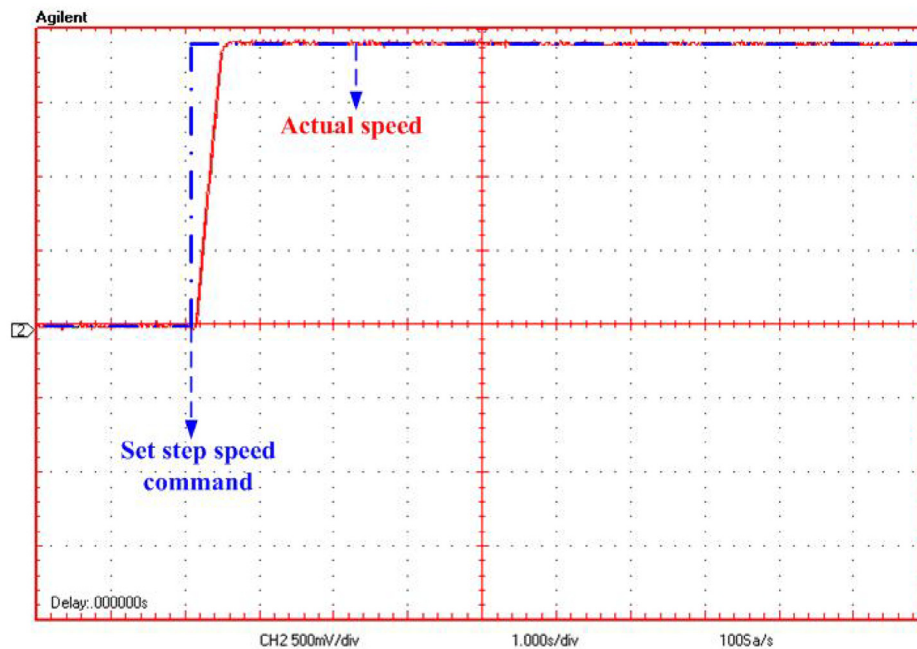


**Fig. 6.** Numerical simulation test, speed behavior of the induction motor controlled by the wavelet-fuzzy IFOC. **Top:** no-load with step decrease in set speed command 183.3-100 rad/sec at  $t = 2.25$  sec, **Middle:** when 30% of rated load is applied at  $t = 3.25$  sec (set speed 183.3 rad/sec), **Bottom:** when 30% of rated load is removed at  $t = 4.25$  sec (set speed 183.3 rad/sec).

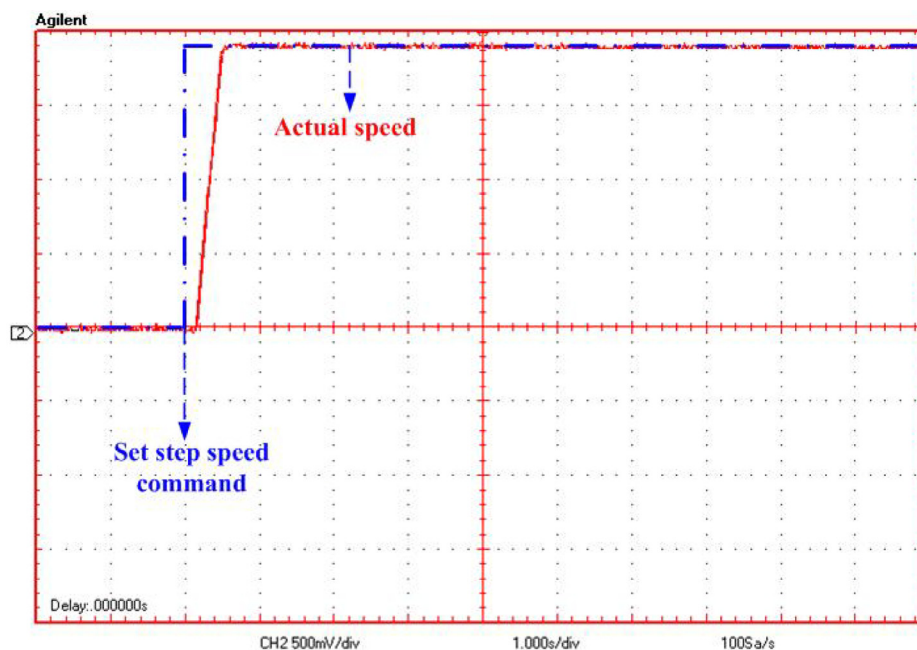
currents of IM are measured by the hall-effect sensors and are supplied to the dsp board. These signals are given as input to the dsp board through the analog/digital converter (ADC) after proper signal conditioning. The proposed compensator generates the torque command for the drive system. The digital output of the dsp control board is used as switching pulses for the inverter. These digital signals are fed through the isolation and driving circuit to trigger the IGBTs of the three-phase inverter. The speed and current signals, obtained by the sensors, are processed by the signal conditioning circuit and then fed to the I/O port of the dsp control board. Tektronix signal

oscilloscope with a bandwidth of 100 MHz and real time sampling rate of 500 mega samples per second (MS/s) is used for tracing the speed behavior.

Table 2 provides the parameters taken for investigation test in both simulation and hardware prototype implementation. Complete numerical model of the proposed wavelet-fuzzy based indirect field oriented controller for induction motor drive is developed in Matlab/Simulink software. The speed response of the ac motor drive is tested under different working condition, in particular, step increment/decrement of speed and load. Further, performance



(a)



(b)

Fig. 7. Prototype experimental test, speed behavior of the induction motor controlled by the wavelet-fuzzy IFOC. (a) Starting at no-load with set speed command 183.3 rad/sec, (b) Starting at loaded condition of 2.5 Nm (set speed 183.3 rad/sec).

indices are set to observe the rise time, peak over shoot, under-shoot, steady state error and root mean square error (RMSE) to prove the effectiveness of the proposed wavelet-fuzzy speed IFOC algorithm. Figs. 5 and 6 shows the complete speed behavior response of the induction motor controlled wavelet-fuzzy performances.

In the first investigation, the transient speed response is illustrated in Fig. 5 (top), where the motor is started at no load with set speed command of 183.3 rad/sec (i.e. the rated speed). In the second investigation, the speed behavior of the induction motor drive is tested, where the initially started with load of 2.5 Nm and a set speed command of 183.3 rad/sec as shown in Fig. 5 (middle). In the third investigation, the speed behavior of the IM drive is tested for step

increase in set speed command speed incremented in step from 100rad/sec to 183.3rad/sec at no load, and it is shown in Fig. 5 (bottom). The speed is increased from 100 rad/sec to 183.3 rad/sec at  $t = 1.0$  sec. Step decremented in set speed command is tested from 183.3rad/sec to 100rad/sec and is shown in Fig. 6 (top) at  $t = 2.25$  sec.

Further, speed behavior response tested under sudden loading of the induction motor is tested and shown in Fig. 6 (middle), where a load is applied at  $t = 3.25$  sec with the set speed command of 183.3rad/sec. Similarly, sudden removal of loading of the induction motor is tested and shown in Fig. 6 (bottom). For this case, the motor is started with the set speed command of 183.3 rad/sec, a

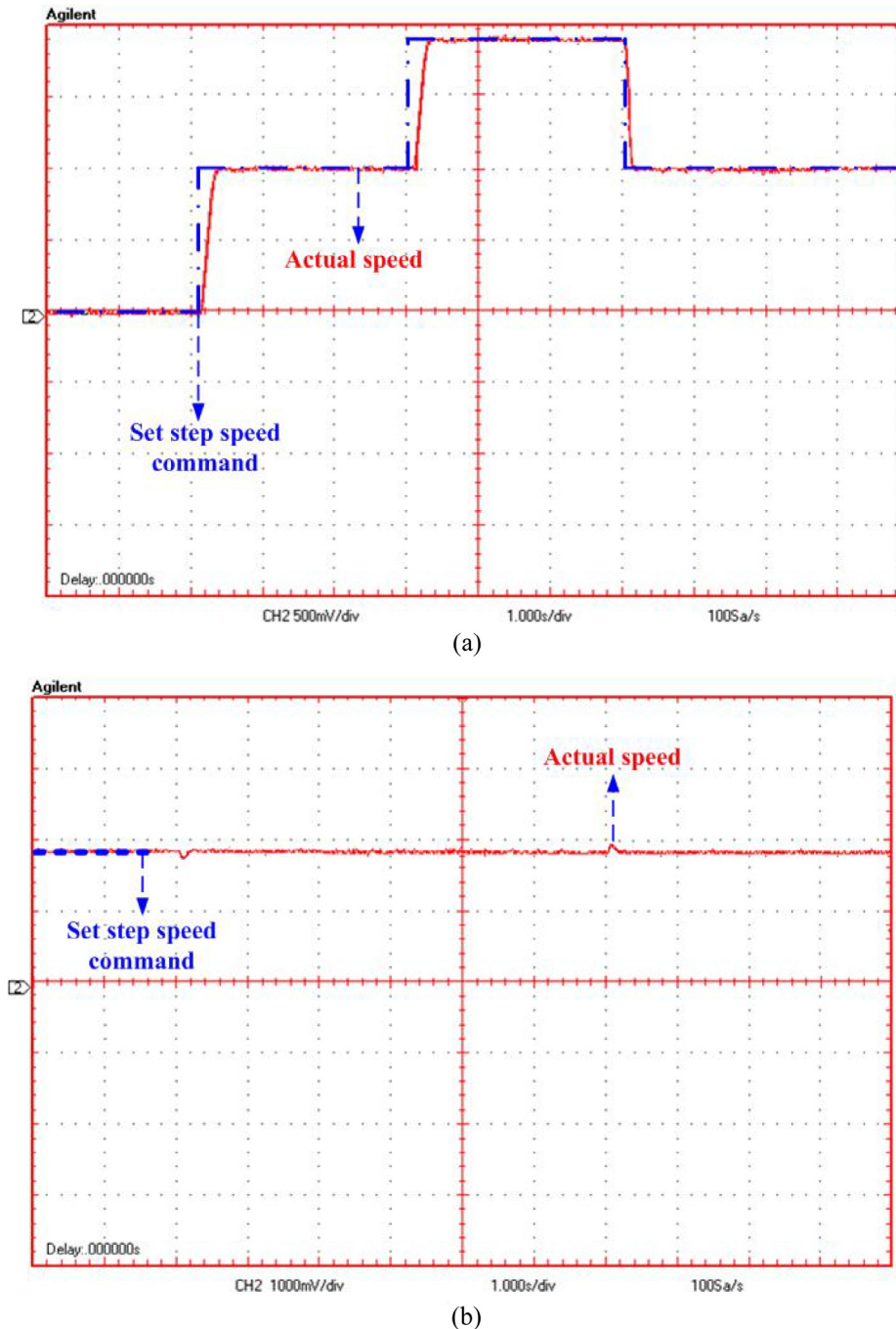


**Fig. 8.** Prototype experimental test, speed behavior of the induction motor controlled by the wavelet-fuzzy IFOC. (a) No-load with step increase in set speed command (0-100-183.3-100 rad/sec at  $t = 2$  sec,  $t = 5$  sec), step decrease in set speed command (183.3-100 rad/sec at  $t = 8$  sec), (b) When step increase in load by 30% of rated load is applied at  $t = 2$  sec and step increase in 30% of rated load (removed) at  $t = 8$  sec (set speed 183.3 rad/sec).



**Table 3**

Observed performances indices of wavelet-fuzzy IFOC controller for IM drive.

Parameter speed	RMSE value	
	Simulation	Experiment
0–183.3 rad/sec	26.32	27.29
100 rad/sec–183.3 rad/sec	15.86	16.38
183.3rad/sec–100 rad/sec	19.21	20.09
180 rad/sec, when load applied 2.5 Nm	31.29	32.46

load of 30% of rated value is applied at  $t = 3.25$  sec, and the load is removed at  $t = 4.25$  sec.

The experimental results for the wavelet-fuzzy technique are shown in Figs. 7 and 8 in comparison to simulation tests. As first investigation, Fig. 6(a) shows the transient speed response at no load with set speed command of 183.3 rad/sec (i.e. the rated speed) of the induction motor.

In second investigation, the induction motor is started with 2.5 Nm loads (30% of rated value) at the start and a set speed command of 183.3 rad/sec as shown in Fig. 6(b). In the third investigation, induction motor is tested for step increment/decrement in set speed command speed from 100rad/sec to 183.3rad/sec to 100rad/sec at no load as at 5 sec, 8 sec and shown in Fig. 7(a) respectively. Finally, the induction motor speed behavior response under sudden loading and removal of load is tested and shown in Fig. 7(b) experimentally, where a load of 2.5 Nm is applied at  $t = 2$  sec, and same load is suddenly removed at  $t = 8$  sec with the set speed command of 183.3rad/sec respectively.

After complete simulation and experimental test investigations, both results obtained thus confirmed the wavelet-fuzzy based controller responded with negligible low peak overshoot, faster rise time, reach steady value in quick approximation and lesser steady state error as per industrial demands. Finally, Table 3 gives the root mean square error (RMSE) values, which shows the good responses under different testing conditions by its value for both simulation and experimental investigation. Further confirms the proposed wavelet-fuzzy controller suitability for the IFOC algorithm for industrial induction motor drive applications.

## 6. Conclusions

Wavelet-fuzzy speed controller for IFOC induction motor drive articulated in this paper with complete system was modeled in numerical simulation software and practically implemented in hardware prototype with dsp TMS320F2812 processor. Set of simulation and experimental investigation results are provided and shown in close conformity with actual expectation. It is confirmed from both numerical and experimental task of investigation that the proposed controller proves the robustness by its response in negligible peak over shoot, faster settling time during transient and minimal steady state error in stable conditions. Further, performance indices on root mean square error (RMSE) values shows good responses, that P-I/P-I-D controller are to be replaced by proposed speed controller for IFOC ac motor drives. Finally, the wavelet-fuzzy controller suits for high precision and accurate speed control of the induction motor which attacks the industrial application needs.

## References

- [1] P. Vas, *Artificial-Intelligence-Based Electrical Machines and Drives Application of Fuzzy, Neural, Fuzzy-Neural, and Genetic-Algorithm-Based Techniques*, 1999. ISBN 978-0-19-859397-3, Hardback.

- [2] P. Sanjeevikumar, J.L. Febin Daya, P.W. Wheeler, F. Blaabjerg, V. Fedák, J.O. Ojo, Wavelet Transform with Fuzzy Tuning Based Indirect Field Oriented Speed Control of Three-Phase Induction Motor Drive. Conf. Proc. The 18th IEEE Intl. Conf. on Electrical Drives and Power Electronics, IEEE-EDPE'15, Slovakia Republic, 21–23 Sep. 2015.
- [3] R.J. Wai, Development of new training algorithms for neuro-wavelet systems on the robust control of induction servo motor drive, IEEE Trans. Ind. Electron. 49 (6) (2002) 1323–1341.
- [4] M.A.S.K. Khan, M. Azizur Rahman, Implementation of a new wavelet controller for interior permanent-magnet motor drives, IEEE Trans. Ind. Appl. 44 (6) (2008) 1957–1965.
- [5] F.J. Lin, P.H. Shen, Y.S. Kung, Adaptive wavelet neural network control for linear synchronous motor servo drive, IEEE Trans. Magn. 41 (12) (2005) 4401–4412.
- [6] H. Yousef, M.E. Elkhatab, O.A. Sebakh, Wavelet network-based motion control of DC motors, Exp. Syst. Appl. 37 (2) (2010) 1522–1527.
- [7] R.J. Wai, H.H. Chang, Backstepping wavelet neural network control for indirect field-oriented induction motor drive, IEEE Trans. on Neural Networks 15 (2) (2004) 367–382.
- [8] S.A. Saleh, M. Azizur Rahman, Analysis and real-time testing of a controlled single-phase wavelet-modulated inverter for capacitor-run induction motors, IEEE Trans. Energy Conv. 24 (1) (2009) 21–29.
- [9] R. Yan, R.X. Gao, Tutorial 21 wavelet transform: a mathematical tool for non-stationary signal processing in measurement science part 2 in a series of tutorials in instrumentation and measurement, IEEE Trans. Instrum. Meas. 12 (5) (2009) 35–44.
- [10] T.K. Sarkar, C. Su, R. Adve, M. Salazar-Palma, L. Garcia-Castillo, R.R. Boix, A tutorial on wavelets from an electrical engineering perspective. I. Discrete wavelet techniques, IEEE Trans. Antennas Propagat. 40 (5) (1998) 49–68.
- [11] V. Vinothkumar, C. Muniraj, Fault diagnosis in h-bridge multilevel inverter drive using wavelet transforms, IJAREEIE 2 (4) (2013).
- [12] H. Liu, P.C. Loh, F. Blaabjerg, Sub-module short circuit fault diagnosis in modular multilevel converter based on wavelet transform and adaptive neuro fuzzy inference system, Electr. Power Compon. Syst. 43 (8–10) (2015) 1080–1088. Taylor and Francis Journal.
- [13] M.A.S.K. Khan, M.A. Rahman, W. Zhang (Ed.), *Wavelet Based Diagnosis and Protection of Electric Motors, Fault Detection*, 2010, doi:10.5772/9068. ISBN: 978-953-307-037-7, InTech.
- [14] R.J. Wai, K.H. Su, Adaptive enhanced Fuzzy Sliding-mode control for Electrical Servo Drives, IEEE Trans. Ind. Electron. 53 (2) (2006) 569–580.
- [15] M. Nasir Uddin, T.S. Radwan, A.M. Rahman, Performances of fuzzy-logic-based indirect vector control for induction motor drive, IEEE Trans. Ind. Appl. 38 (5) (2002) 1219–1225.
- [16] S. Parvez, Z. Gao, A wavelet based Multiresolution PID controller, IEEE Trans. Ind. Appl. 41 (2) (2005) 537–543.
- [17] J.L. Febin Daya, V. Subbiah, P. Sanjeevikumar, Robust speed control of an induction motor drive using wavelet-fuzzy based self-tuning multi-resolution controller, Int. J. Comput. Intell. Syst. 6 (4) (2013) 724–738.
- [18] A. Nejadpak, A. Mohamed, O.A. Mohammed, A.A. Khan, Online Gain Scheduling of Multiresolution Wavelet based Controller for acoustic noise and Vibration reduction in sensorless control of PM synchronous motor at low speed, in Proc. IEEE Power and Energy meeting, Michigan, USA, 2011.
- [19] G. Stang, T. Nguyen, *Wavelet and Wavelet Filter BANKS*, Wellesley-Cambridge Press, Wellesley, 1997.
- [20] E.Y. Hamid, Z.I. Kawasaki, Wavelet-based data compression of power system disturbances using the minimum description length criterion, IEEE Trans. Power Deliv. 17 (2) (2002) 460–466.
- [21] M. Khan, M.A. Rahman, A Novel neuro-wavelet-based self-tuned wavelet controller for IPM motor drives, IEEE Trans. Ind. Appl. 46 (3) (2010) 1194–1203.
- [22] J.L. Febin Daya, P. Sanjeevikumar, F. Blaabjerg, P.W. Wheeler, O. Ojo, Implementation of wavelet based robust differential control for electric vehicle application, IEEE Trans. Power Elect. (2015) doi:10.1109/TPEL.2015.2440297.
- [23] P. Sanjeevikumar, J.L. Febin Daya, F. Blaabjerg, N. Mir-Nasiri, A.H. Ertas, Numerical implementation of wavelet and fuzzy transform IFOC for three-phase induction motor, JESTECH (2015) doi:10.1016/j.jestech.2015.07.002 Elsevier Journal Publications.
- [24] J.L. Febin Daya, V. Subbiah, A. Iqbal, P. Sanjeevikumar, A novel wavelet-fuzzy based indirect field oriented control of induction drives, J. Power Electron. 13 (4) (2013) 656–668 The Korean Institute of Power Electronics, Seoul (Republic of Korea).
- [25] J.L. Febin Daya, P. Sanjeevikumar, F. Blaabjerg, P. Wheeler, O. Ojo, A.H. Ertas, Analysis of wavelet controller for robustness in electronic differential of electric vehicles – an investigation and numerical implementation, Electr. Power Compon. Syst. (2015) Taylor and Francis Publications, Accepted for publication.